Bull. Soc. géol. Fr., 2008, t. 179, n° 5, pp. 445-452

Late Jurassic continental flood basalt doleritic dykes in northwestern Cuba: remnants of the Gulf of Mexico opening

JAMES ALLIBON[1,2], HENRIETTE LAPIERRE[†], FRANÇOIS BUSSY[1], MARC TARDY[3], ESTHER M. CRUZ GÀMEZ[4] and FRANÇOIS· SENEBIER[2]

Key-words. – Dolerite dykes, Upper Jurassic, Continental flood basalts, Geochemistry, Cuba.

Abstract. – Accreted terranes, comprising a wide variety of Late Jurassic and Early Cretaceous igneous and sedimentary rocks are an important feature of Cuban geology. Their characterization is helpful for understanding Caribbean paleogeography.

The Guaniguanico terrane (western Cuba) is formed by upper Jurassic platform sediments intruded by microgranular dolerite dykes. The geochemical characteristics of the dolerite whole rock samples and their minerals (augitic clinopyroxene, labradorite and andesine) are consistent with a tholeiitic affinity. Major and trace element concentrations as well as Nd, Sr and Pb isotopes show that these rocks also have a continental affinity. Sample chemistry indicates that these lavas are similar to a low Ti-P_2O_5 (LTi) variety of continental flood basalts (CFB) similar to the dolerites of Ferrar (Tasmania). They derived from mixing of a lithospheric mantle source and an asthenopheric component similar to E-MORB with minor markers of crustal contamination and sediment assimilation. However, the small quantity of Cuban magmatic rocks, similarly to Tasmania, Antarctica and Siberia differs from other volumetrically important CFB occurrences such as Parana and Deccan.

These dolerites are dated as 165-150 Ma and were emplaced during the separation of the Yucatan block from South America. They could in fact be part of the Yucatan-South America margin through which the intrusive system was emplaced and which was later accreted to the Cretaceous arc of central Cuba and to the Palaeogene arc of eastern Cuba. These samples could therefore reflect the pre-rift stage between North and South America and the opening of the gulf of Mexico.

L'existence de filons tardi-jurassiques de trapps continentaux dans le nord-ouest de Cuba : témoins de l'ouverture du golfe du Mexique

Mots-clés. – Filons doléritiques, Jurassique supérieur, Trapps continentaux, Géochimie, Cuba.

Résumé. – La géologie de l'île de Cuba est caractérisée par l'existence de terrains accrétés composés d'une grande variété de roches ignées et sédimentaires d'âge jurassique supérieur et crétacé inférieur. L'identification de la nature de ces terrains est fondamentale pour la compréhension de la paléogéographie du domaine caraïbe.

La formation de Guaniguanico (N-Ouest Cuba) est constituée de sédiments de plate-forme d'âge jurassique supérieur recoupés par des filons doléritiques. Les caractéristiques géochimiques de ces dolérites et des minéraux qu'elles contiennent (augite et labrador) permettent de mettre en évidence l'affinité tholéiitique de ces roches. Les concentrations en éléments majeur et traces ainsi que les rapports isotopiques du Pb, Sr et Nd indiquent que ces dolérites présentent des signes de contamination crustale et d'assimilation des sédiments encaissants. L'étude géochimique de ces filons doléritiques montre que ces laves sont proches d'une variété de trapps continentaux pauvres en TiO_2 et P_2O_5 (LTi), similaire aux dolérites de Ferrar (Tasmanie), elles-mêmes dérivées du mélange d'une source de type manteau lithosphérique avec une source de type manteau asthénosphérique appauvri (type E-MORB). Le faible volume de roches trouvées à Cuba tout comme en Tasmanie, en Antarctique et en Sibérie diffère fortement des grands volumes de trapps émis au Deccan ou au Parana.

Les dolérites cubaines sont datées à 165-150 Ma et sont associées à la séparation du bloc Yucatan de l'Amérique du Sud. Elles se seraient mises en place à travers la marge passive Yucatan-Amérique du Sud, ultérieurement accrétée aux arcs Crétacé et Paléogène du centre et de l'est de Cuba. Ces roches pourraient donc refléter la phase précoce du rifting entre l'Amérique du Nord et l'Amérique du Sud et donc l'ouverture du golfe du Mexique.

1. Institut de Minéralogie et de Géochimie, Université de Lausanne, Bât Anthropole, CH1015, Lausanne, Switzerland.
2. LGCA, UMR CNRS 5025, Maison des Géosciences, Université Joseph Fourier Grenoble 1, 1381 rue de la piscine, 38041 Grenoble, France.
3. LGCA, UMR CNRS 5025, Université de Savoie, F.73376 Le Bourget du Lac, France
4. Universidad Autonoma de Nuevo Léon, Facultad de Ciencias de la Tierra, Carr. A Cerro Prieto km 8, ex-hacienda de Guadelupe, CP 67700, A P 104, Linares, Nuevo Leon, Mexico.
Manuscrit déposé le 14 février 2007; accepté après révision le 14 septembre 2007

INTRODUCTION

Previous studies [Iturralde-Vinent 1994, 1996a, 1998; Kerr *et al.*, 1999; Maresch *et al.,* 2000; Blein *et al.*, 2003] focused on the Cretaceous and Palaeogene arc-suites of central and eastern Cuba. These subduction-related rocks bring new insight on the geodynamic implications concerning the subduction of the Pacific beneath Central America and help understand the effects of the thick and buoyant Late Cretaceous Caribbean plateau [CCOP, Kerr *et al.*, 1996, 1997; Sinton *et al.,* 1998; Lapierre *et al.*, 2000] on this subduction zone. However, all the Mesozoic Cuban rocks do not display arc-affinities. Indeed, the geochemical study of mafic dykes intruding Jurassic turbidites [Reguera *et al.*, 1999] exposed in the Sierra del Rosario reveals the presence of within-plate tholeiitic magmatism [Kerr *et al.*, 1999]. These mafic dykes found in the El Sábalo Formation differ from other Cuban basalts in terms of both their thickness (~ 400 m) and their age (Oxfordian-Early Kimmeridgian) and intrude deformed continental margin type Jurassic turbidites.

Despite the poor and limited exposures of the El Sábalo tholeiitic dykes, these rocks are important to depict the geodynamic history of the intra-American area during Jurassic times. This detailed geochemical study on whole-rock and clinopyroxene separates from the mafic dykes allows us to identify their magmatic affinities and mantle sources. These geochemical data help constrain an event of the geodynamic evolution of the intra-American area, i.e., the opening of the Gulf of Mexico.

GEOLOGICAL SETTING

Cuba belongs to the northwestern Caribbean region, its study is fundamental to the understanding of the Mesozoic-Cenozoic plate movements in the area. The island of Cuba is bounded, to the south, by the Cayman-Bartlett trench. This major sinistral transform fault separates the North American and Caribbean plates and protected Cuba from the major post-Palaeogene shearing that overprinted the earlier tectonic events in most of the Greater Antilles.

The island of Cuba (fig.1) can be divided into three main geological domains based on stratigraphy, type of magmatic activity and tectonic style: the West Cuban nappe stack, the central Cuban main thrust belt and the south-eastern Cretaceous and Palaeogene arcs. Each one is separated from the other by NE-SW trending faults [Iturralde-Vinent, 1994, 1996a, 1996b; Meschede and Frisch, 1998, 2002; Kerr *et al.*, 1999; Muller *et al.*, 1999; Maresch *et al.*, 2000; Rodriguez *et al.*, 1997; Stanek *et al.*, 2000].

Three structurally and lithologically complex allochthonous terranes are present in south-central and western Cuba

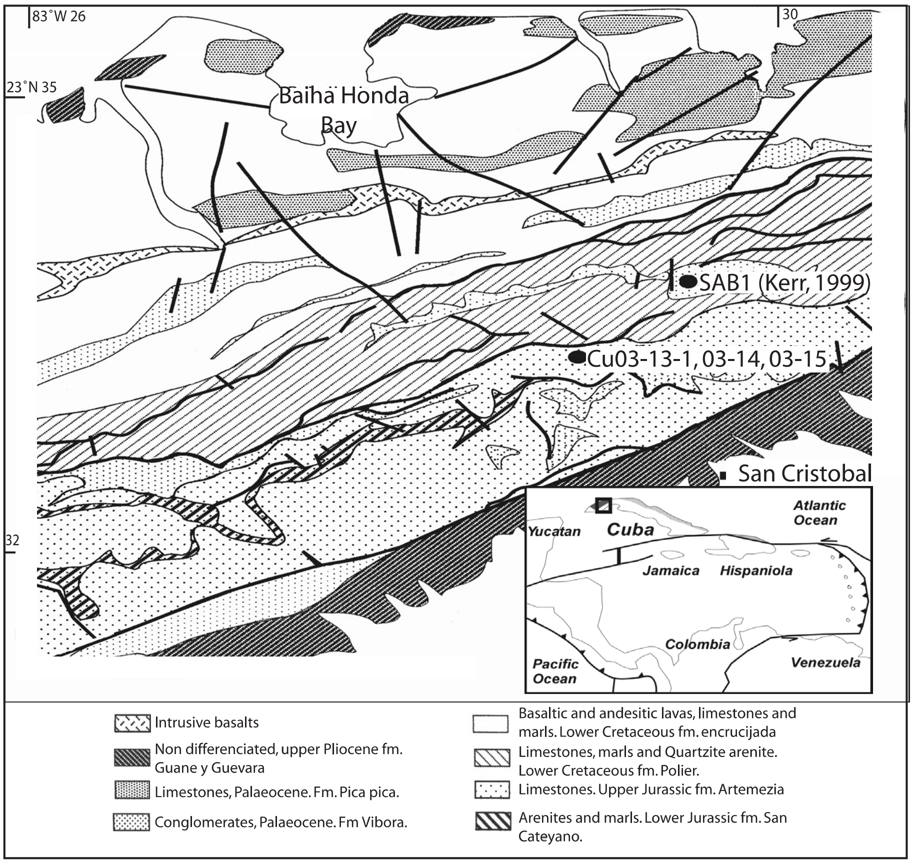

FIG. 1. – Revised general map of Cuba showing main lithological units and pre-late Eocene northern passive margin outcrops [Rodríguez *et al.*, 1997] and detailed map of the geology of Cuba from the Bahia Honda bay to San Cristobal showing the location of the analyzed samples, subject of this work. SAB1 is the sample described by Kerr *et al.* [1999].
FIG. 1. – *Carte générale modifiée de Cuba montrant les principales unités lithologiques ainsi que les affleurements de la marge passive éocène. [Rodríguez* et al., *1997] et carte géologique détaillée de la zone comprise entre la baie de Bahia Honda et San Cristobal montrant la position des échantillons traités dans ce papier.* SAB1 *est un échantillon décrit par Kerr* et al. *[1999].*

(Guaniguanico, Escambray and Pinos [Iturralde-Vinent, 1994]). They expose Jurassic-Cretaceous sediments of continental margin type as well as ophiolitic rocks and Cretaceous volcanic arc suites. In the Guaniguanico terrane, Paleocene to lower Eocene foreland sediments can also be found. There is strong evidence that all three terranes were originally located along the eastern margin of the Maya block (Yucatan platform, [Iturralde-Vinent, 1994]) and were preserved as tectonic windows in Cretaceous arc rocks as shown by the existence of mafic dykes in Jurassic sediments. These mafic dykes and their host sediments are strongly metamorphosed in the Pinos and Escambray terranes (high pressure-low temperature [Kerr *et al.*, 1999]), but are much less affected in the Guaniguanico terrane [Schneider *et al.*, 2004].

The studied area corresponds to the Guaniguanico massif (fig. 1). This terrane consists of a stack of several NE-SW trending thrust units [Iturralde-Vinent, 1994]. The lower units, Los Organos and Rosario Belts (Rosario South, Rosario North and Quiñones) consist of Early Jurassic to late Cretaceous sedimentary rocks [Pszczolkowski, 1978], whereas the upper units consist of serpentinites, gabbros and Cretaceous igneous and sedimentary rocks of the Felicidades belt [Iturralde-Vinent, 1994]. The three samples analysed in this paper were collected in the vicinity of 'Los Tumbos', north of San Cristobal, and belong to the mafic El Sábalo Formation in the South Rosario belt. They belong to a series of mafic dykes that intrude the Upper Jurassic-Lower Cretaceous platform sediments and limestones. The sediments crosscut by the mafic dykes are paleontologically dated to late Oxfordian-early Kimmeridgian [Reguera *et al.*, 1999].

ANALYTICAL PROCEDURES

Wavelength-dispersive analyses for clinopyroxene major-element compositions were made on a Cameca SX-50 electron microprobe fitted with five spectrometers at the Institute of Mineralogy and Geochemistry of the University of Lausanne. The standard procedures are 15 kV and 20 nA with an electron beam of 1 µm width and integrated counting times of 15 on background and 30 s on the peak. Synthetic and natural minerals were used as standards. A computer correction program (PAP) was used to calculate the element concentrations. The accuracy of major element determinations is better than ± 5% of the total values.

Trace element measurements on minerals were made by laser-ablation ICP-MS mass spectrometry using an Ar-F 193 nm Lambda Physik© Excimer laser coupled with a Perkin-Elmer 6100DRC ICP-MS at the Institute of Mineralogy and Geochemistry of the University of Lausanne. NIST610 and 612 glasses were used as external standards, Ca as internal standards after microprobe measurements on the pit sites. Ablation pit size varied from 40 to 80 nm. BCR2 basaltic glass was regularly used as a monitor to check for reproducibility and accuracy of the system. Results were always within ± 10% of the certified values.

Major- and trace-element concentrations were measured by ICP-AOS at the Université de Bretagne Occidentale, Brest, following Cotten *et al.*'s [1995] procedures. Complementary trace element concentrations were measured by ICP-MS at the Université Joseph Fourier, Grenoble, following Barrat *et al.*'s [1996] procedures.

Sr (static acquisition) and Nd (dynamic acquisition) isotopic ratios were measured at the Laboratoire de Géochimie isotopique de l'Université Paul Sabatier, Toulouse, on a Finnigan MAT261 multicollector mass spectrometer using the analytical procedures described by Lapierre *et al.* [1997]. Results on standards yielded $^{143}Nd/^{144}Nd = 0.511850 \pm 0.000017$ (2σ external reproducibility) on 12 standards analysed. Results on NBS 987 Sr standard yielded $^{87}Sr/^{86}Sr = 0.710250 \pm 0.000030$ (2σ external reproducibility) on 11 standard determinations. $^{87}Sr/^{86}Sr$ and $^{143}Nd/^{144}Nd$ were normalized for mass fractionation relative to $^{86}Sr/^{88}Sr = 0.1194$ and $^{146}Nd/^{144}Nd = 0.7219$ respectively. εNd_i was calculated with actual $(^{143}Nd/^{144}Nd)_{CHUR} = 0.512638$ and $(^{147}Sm/^{144}Nd)_{CHUR} = 0.1967$. εSri was calculated with actual $(^{87}Sr/^{86}Sr)_{CHUR} = 0.70450$ and $(^{87}Rb/^{86}Sr)_{CHUR} = 0.084$ [McCulloch and Wasserburg, 1978].

For lead separation, powdered samples were weighed to obtain approximately 200 ng of lead. Samples were leached with 6N HCl during 30 minutes at 65°C before acid digestion. They were dissolved for 48 hours on a hotplate in a tri-distilled HF/HNO_3 mixture. After evaporation to dryness, 1 ml of HNO_3 was added to the residue and kept at about 90°C for 12-24 h. After complete evaporation, 0.5 ml of 8N HBr was added to the sample, which was kept at 70°C for 2-3 h before complete evaporation. The chemical separation of lead was done using 50 µl of anion exchange resin (AG1X8, 200-400 mesh) and samples were loaded and washed in 0.5N HBr. Lead was then eluted in 6N HCl. Pb blanks were less than 40 pg and are negligible for the present analyses.

Lead isotopes were analysed on a VG Plasma 54 multicollector inductively coupled plasma mass spectrometer (MC-ICP-MS) at the Ecole Normale Supérieure de Lyon. Lead isotope compositions were measured using the Tl normalization method [White *et al.*, 2000]. For Pb isotope analysis, samples were bracketed between NIST 981 standard measurements and calculated with respect to the value reported for this standard [Todt *et al.*, 1996].

All isotopic data are corrected for in situ decay using an age of 150 Ma [Kerr *et al.*, 1999].

PETROLOGY AND MINERAL CHEMISTRY OF THE DOLERITES

All three doleritic samples show an intersertal texture formed by plagioclase laths (40 vol. %, An 45-60) surrounded by clinopyroxene (15 vol. %). The groundmass consists of interstitial secondary minerals (*i.e.*, chlorite and serpentinite) and oxides. Preserved sub-rectangular and sub-octagonal clinopyroxene occur either as single crystals or as slightly altered aggregates. Euhedral plagioclase occurs in elongated isolated laths or as radial aggregates. Samples contain an important number of subhedral oxides (10 vol.%), which are mostly ilmenite, with rare magnetite and pyrite. Serpentine and chlorite can be found as alteration products in veins and fractures formed during weathering.

Clinopyroxenes show zoned augitic compositions ($Wo_{39.8-26.7}$, $En_{47.8-29.89}$, $Fs_{30.51-14.73}$; [Morimoto *et al.*, 1988]) (fig.2) and have low Ti values (0.01 pfu to 0.02 pfu) for Ca values < 0.8 (pfu) which is typical of tholeiitic

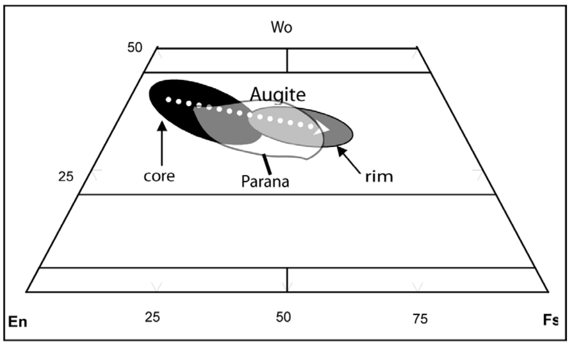

FIG. 2. – Clinopyroxene composition and classification diagram [Morimoto *et al.*, 1998]. Values for CFB Parana clinopyroxenes are from Pik *et al.* [1998].
FIG. 2. – *Diagramme de nomenclature des clinopyroxenes [Morimoto* et al.*, 1998]. Les compositions des clinopyroxenes de Parana sont de Pik* et al. *[1998].*

clinopyroxenes [Leterrier *et al.*, 1982] (table I). Chemical variations within clinopyroxene phenocrysts can also be seen when opposing FeO, CaO, TiO_2 and Cr_2O_3 concentrations (fig. 3) to the XMg (= Mg/(Mg+Fe)). Indeed, crystal cores are FeO- and TiO_2-enriched in comparison to the CaO- and Cr_2O_3-enriched rims, this is typical of

TABLE I. – Major element (wt.%) for most representative Cu 03.15 clinopyroxene mineral samples. Structural formulae are calculated on the basis of 6 oxygens.
TABL. I. – *Concentrations en éléments majeurs (wt.%) pour les grains de clinopyroxènes les plus représentatifs de l'échantillon Cu.03.15. La formule structurale est calculée sur une base de 6 oxygènes.*

Label	1	2	1'	3	4	5	6	2'	3'
	core	core	rim	core	core	core	core	rim	rim
SiO_2	52.07	51.66	50.36	51.95	52.07	49.91	51.83	52.06	52.05
TiO_2	0.54	0.55	0.79	0.58	0.58	0.63	0.64	0.55	0.56
Al_2O_3	2.02	1.87	1.46	1.89	1.72	1.05	2.76	1.98	1.38
Cr_2O_3	0.03	0.03	0.04	0.03	0.02	0.01	0.04	0.04	0.02
Fe_2O_3(c)	0.66	1.64	1.65	0.90	0.23	1.37	0.86	0.89	0.00
FeO(c)	10.88	8.81	15.46	9.88	11.75	22.46	8.99	9.44	18.67
MnO	0.37	0.25	0.40	0.31	0.30	0.64	0.27	0.27	0.50
MgO	16.48	15.68	12.25	15.60	14.73	9.85	15.57	15.76	14.67
CaO	16.57	18.86	17.09	18.33	18.25	14.60	18.97	18.65	12.79
Na_2O	0.19	0.24	0.29	0.25	0.24	0.19	0.27	0.23	0.16
Sum	99.82	99.59	99.78	99.74	99.88	100.72	100.20	99.86	100.79
Si	1.94	1.93	1.93	1.94	1.95	1.94	1.92	1.94	1.96
Ti	0.02	0.02	0.02	0.02	0.02	0.02	0.02	0.02	0.02
Al/AlIV	0.06	0.07	0.07	0.06	0.05	0.05	0.08	0.06	0.04
AlVI	0.03	0.01	0.00	0.02	0.03	0.00	0.04	0.02	0.02
Cr	0.00	0.00	0.00	0.00	0.00	0.00	0.00	0.00	0.00
Fe^{3+}	0.02	0.05	0.05	0.03	0.01	0.04	0.02	0.03	0.00
Fe^{2+}	0.34	0.28	0.50	0.31	0.37	0.73	0.28	0.29	0.59
Mn^{2+}	0.01	0.01	0.01	0.01	0.01	0.02	0.01	0.01	0.02
Mg	0.91	0.87	0.70	0.87	0.82	0.57	0.86	0.87	0.82
Ca	0.66	0.75	0.70	0.73	0.73	0.61	0.75	0.74	0.52
Na	0.01	0.02	0.02	0.02	0.02	0.01	0.02	0.02	0.01
Sum Cat#	4.00	4.00	4.00	4.00	4.00	4.00	4.00	4.00	4.00
Wo(Ca)	34.53	39.66	36.99	38.39	38.09	31.86	39.81	38.90	26.78
En(Mg)	47.78	45.87	36.88	45.46	42.77	29.89	45.46	45.73	42.71
Fs(Fe^{2+})	17.70	14.47	26.13	16.15	19.14	38.25	14.73	15.36	30.51

TABLE II. – Trace-element concentrations (ppm) for most representative Cu 03.15 clinopyroxene mineral grains.
TABLE. II. – *Concentrations en éléments traces (ppm) pour les grains de clinopyroxènes les plus representatifs de l'échantillon Cu.03.15.*

Sample	Cpx1	Cpx2	Cpx3
Rb	-	0.02	0.03
Ba	0.01	0.03	0.19
Th	0.00	0.00	-
U	0.00	0.00	0.00
Nb	-	0.00	0.00
Ta	0.01	0.00	0.00
La	0.18	0.10	0.08
Ce	1.04	0.58	0.44
Pb	0.01	0.06	0.05
Sr	3.88	3.35	13.45
Nd	2.86	1.53	0.94
Sm	1.80	0.98	0.59
Zr	10.01	4.97	2.65
Hf	0.58	0.29	0.16
Eu	0.64	0.40	0.25
Gd	-	-	-
Tb	0.77	0.41	0.22
Dy	6.31	3.29	1.69
Y	34.77	19.00	9.66
Er	3.73	2.13	1.11
Yb	3.94	2.15	1.07
Lu	0.65	0.16	-

clinopyroxenes with a tholeiitic affinity. Clinopyroxene rare earth element (REE, table II) patterns normalised to chondrites [Sun and McDonough, 1989] (fig.5) are depleted in light (L) REE and show Eu (Eu/Eu* < 0.9) negative anomalies linked to plagioclase removal. Primitive mantle normalised-spidergrams [Sun and McDonough, 1989] (fig. 4) show low and variable concentrations in large ion lithophile elements (LILE, Rb, Ba), U and Pb. This could reflect trace element mobility due to the alteration or low grade metamorphism experienced by these dykes. Clinopyroxene spidergrams are also characterized by marked Nb, Ta, Zr and Hf negative anomalies.

MAJOR AND TRACE ELEMENT CHEMISTRY

The analyzed samples are similar to oceanic tholeiites in terms of major-element chemistry as shown by low alkali index [Middlemost *et al.*, 1975, AI = $(Na_2O + K_2O)/(SiO_2-43) \times 0.17$] (2 to 3) and Al_2O_3 (13-15 wt.%) values (table III).

Tholeiitic flood basalts are closely similar to oceanic tholeiites (MORB and Oceanic Island Basalt, OIB) in terms of major-element chemistry. Similarly to CFBs, the Cuban samples have low Ni (32 to 52 ppm) and Cr (12 to 99 ppm) values. These rocks are Ni-poor and have relatively low Mg values ($Mg/(Mg + Fe_t) < 0.7$). Despite this tholeiitic nature illustrated by $Na_2O + K_2O < 4$ and SiO_2 of 48 to 50 wt.% [Le Maitre *et al.*, 1989], the low MgO concentrations (< 8 wt.%) suggest that these magmatic rocks are not

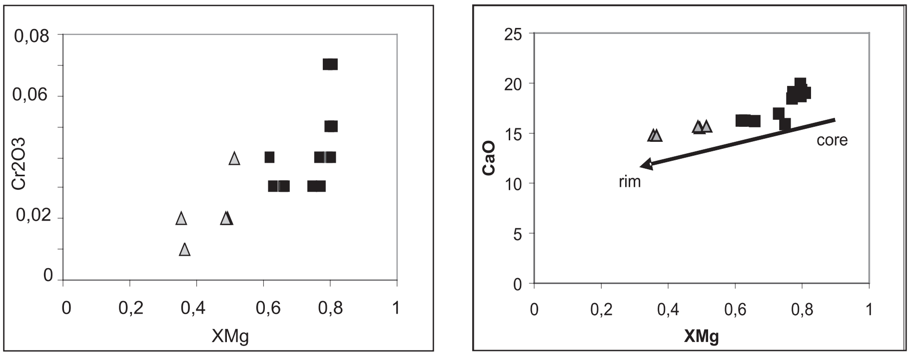

FIG. 3. – Cu 03.15 Clinopyroxene binary correlation diagrams, plotting major elements (wt.%) vs. XMg (XMg = MgO/(MgO+FeO)).
FIG. 3. – *Diagrammes binaires de corrélation des compositions des clinopyroxènes de l'échantillon Cu.03.15 en éléments majeurs (wt.%) vs. XMg (XMg = Mg/(Mg+Fe)).*

TABLE III. – Whole rock major- (wt.%), trace-element (ppm) and Nd and Pb isotopic compositions. Total iron is shown as Fe_2O_3.
TABL. III. – *Concentrations en elements majeurs (wt.%), éléments traces (ppm) et rapports isotopiques des échantillons Cu.03.13.1, Cu.03.14 et Cu.03.15. Le fer total est indiqué* Fe_2O_3.

		Cu03.13.1	Cu03.14	Cu03.15
		dolerite	dolerite	dolerite
SiO_2	wt%	50	49.7	48.2
TiO_2	wt%	1.06	1.13	1.04
Al_2O_3	wt%	13.2	13.65	14.75
Fe_2O_3	wt%	10.4	12.85	12.25
MnO	wt%	0.18	0.2	0.21
MgO	wt%	6.97	7.11	7.42
CaO	wt%	10.05	10.4	10.85
Na_2O	wt%	3.65	2.27	2.2
K_2O	wt%	0.13	0.05	0.07
P_2O_5	wt%	0.08	0.08	0.08
LOI	wt%	3.91	2.19	2.24
Total	wt%	99.6	99.63	99.31
Sc		48	49	43
Ti	ppm	6360	6780	6240
V	ppm	332	347	308
Ni	ppm	39	32	54
Co	ppm	43.22	45.879	53.341
Cr	ppm			
Cs	ppm	0.38	0.09	0.15
Rb	ppm	2.6	0.71	1.239
Ba	ppm	21.96	9.69	12.653
Th	ppm	0.09	0.07	0.059
U	ppm	0.02	0.02	0.015
Nb	ppm	0.75	0.65	0.652
Ta	ppm	0.05	0.05	0.039
Pb	ppm	15.72	0.62	0.471
Sr	ppm	214.91	92.43	94.309
Zr	ppm	55.31	58.81	57.545
Hf	ppm	1.56	1.65	1.538
Y	ppm	28.83	33.51	31.868
La	ppm	1.17	1.34	1.345
Ce	ppm	4.44	5.04	5.039
Pr	ppm	0.85	0.96	0.943
Nd	ppm	5	5.79	5.62
Sm	ppm	2.17	2.41	2.253
Eu	ppm	0.8	0.94	0.902
Gd	ppm	3.26	3.68	3.387
Tb	ppm	0.63	0.73	0.692
Dy	ppm	4.44	5.09	4.559
Ho	ppm	1.02	1.14	1.045
Er	ppm	3.03	3.37	3.137
Tm	ppm	nd	nd	nd
Yb	ppm	3.1	3.38	3.056
Lu	ppm	0.47	0.53	0.458
$^{87}Sr/^{86}Sr$		0.707305 ± 5	0.704761 ± 5	0.704772 ± 5
$^{87}Rb/^{86}Sr$		0.350552	0.038773	0.021868
(e Sr)i		42.3	6.2	6.4
$^{143}Nd/^{144}Nd$		0.513191	0.513176	0.513179
$^{147}Sm/^{144}Nd$		0.255615	0.262203	0.24207
$(^{143}Nd/^{144}Nd)i$		0.51294	0.512919	0.512941
(eNd)i		9.7	9.2	9.7
$(^{206}Pb/^{204}Pb)$		19.34	18.64	18.78
$(^{207}Pb/^{204}Pb)$		15.68	15.6	15.67
$^{208}Pb/^{204}Pb)$		38.47	38.35	38.57

primitive in nature and may have undergone fractionation, as shown by the low Ni values (olivine fractionation). At similar MgO contents, these dolerites show low TiO_2 (< 1.13 wt.%) and P_2O_5 (0.08 wt.%) concentrations and are similar to a low-P_2O_5-Ti variety of flood basalts [Gibson *et al.*, 1995; Pik *et al.*, 1998]. In the Nb/La vs. Ti/Y plot (fig. 6) we can clearly see that the chemistry of these rocks is close to the LTi Parana and Ethiopia CFBs.

Chondrite-normalised REE diagrams for the Cuban Jurassic dolerites exhibit MORB-like characteristics (LREE depletion, flat HREE patterns, fig. 4). Primitive mantle normalised-spidergrams [Sun and McDonough, 1989] (fig. 5) show that the dolerites are depleted in incompatible elements but enriched in Rb, Ba (LILE). This LILE enrichment likely reflects alteration and/or low grade metamorphism. The spidergrams are very flat towards the less incompatible elements but exhibit small Pb and Sr negative anomalies with the exception of sample Cu03-13-1. The latter, collected at the dykes chilled margin, differs from the other samples by its marked Pb and Sr positive anomalies.

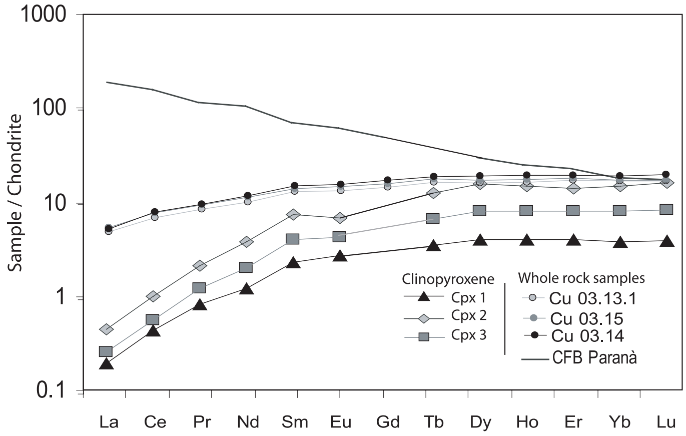

FIG. 4. – Chondrite normalised REE patterns for whole rock and clinopyroxene samples [Sun and Mc Donough, 1989]. Values for CFB Parana are from Pik *et al.* [1998].
FIG. 4. – *Spectres des terres rares normalisés aux chondrites [Sun et Mc Donough, 1989] des échantillons Cu.03.13.1, Cu.03.14 et Cu.03.15 ainsi que des clinopyroxènes de l'échantillon Cu.03.15. Les spectres des roches de Parana sont de Pik* et al. *[1998].*

ND, SR AND PB ISOTOPIC CHEMISTRY

The three doleritic samples show very homogeneous Nd isotopic compositions with εNd values of +9 (table III), indicating a rather depleted mantle source. Cu03-13.1 clinopyroxene separates have a slightly lower εNd of +8.5.

Initial $(^{87}Sr/^{86}Sr)_i$ ratios vary from 0.705424 to 0.705614 (table III) and do not correlate with the εNd values. In the εNd vs. $(^{87}Sr/^{86}Sr)_i$ correlation diagram (not presented here), the dolerites do not fall in the Mantle Array and shift towards high $(^{87}Sr/^{86}Sr)_i$ values. This suggests that the Rb-Sr isotope system has been modified by the alteration and/or low grade metamorphism that affects the Cuban Jurassic dolerites.

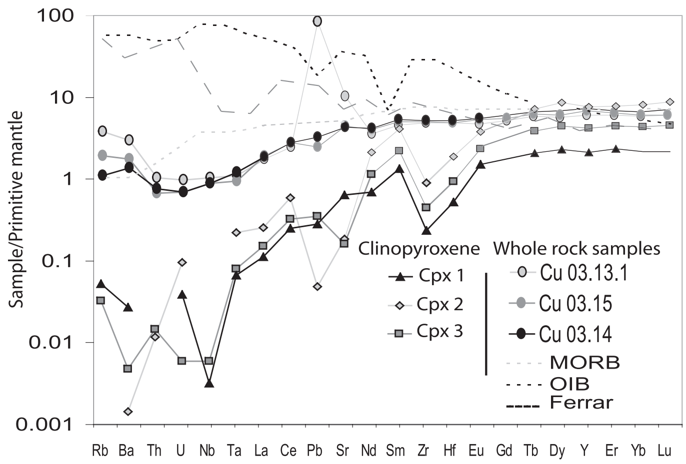

FIG. 5. – Primitive mantle normalised multi-element spidergrams for whole rock and clinopyroxene samples [Sun and Mc Donough, 1989]. MORB and OIB patterns are from Hofmann [1988], The Ferrar pattern is from Hergt *et al.* [1989].
FIG. 5. – *Spectres multi-élémentaires normalisés au manteau primitif [Sun et Mc Donough, 1989] des échantillons Cu.03.13.1, Cu.03.14 et Cu.03.15 ainsi que des clinopyroxènes de l'échantillon Cu.03.15. Les spectres des MORB et OIB sont de Hofmann [1998], celui de Ferrar est de Hergt* et al. *[1989].*

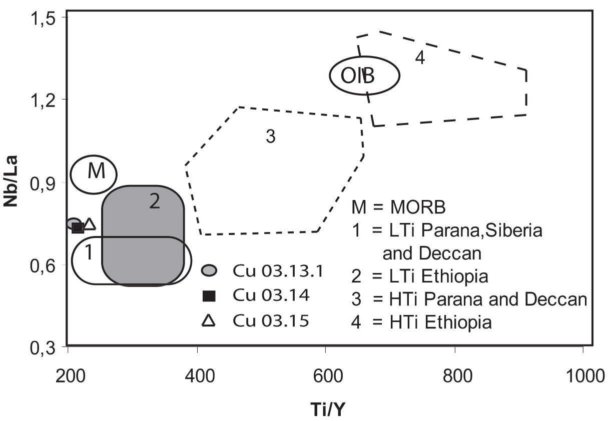

FIG. 6. – Whole rock Nb/La vs. Ti/Y diagram after Pik *et al.* [1998].
FIG. 6. – *Diagramme binaire Nb/La vs. Ti/Y pour les échantillons Cu.03.13.1, Cu.03.14 et Cu.03.15* [Pik *et al.*, 1998].

In the ($^{208}Pb/^{204}Pb$)i-($^{206}Pb/^{204}Pb$)i correlation diagram (fig. 7), the dolerite sampled in the dyke margin falls within the MORB field while the two others are in the OIB and low P_2O_5-TiO_2 basalt fields. In the ($^{207}Pb/^{204}Pb$)i vs. ($^{206}Pb/^{204}Pb$)i diagram (fig. 8), two samples cluster in the EM2 field while the sample collected in the chilled margin falls in the Upper Continental Crust field.

DISCUSSION

Samples studied in this paper are part of the Guaniguanico formation of N-W Cuba and are identified as continental margin rift tholeiites, dated as Oxfordian to early Kimmeridgian, that were formed during the separation of the Yucatan (Mayan block) from northern South America [Kerr *et al.*, 1999]. In this unit Kerr *et al.* [1999] described a sample referred to as basalt from el Sabalo Fm. (SAB1, fig. 1) with geochemical similarities to the samples described in this paper.

The low alkali index of these dolerite samples [Middlemost, 1975] (AI=2 to 3) and Al_2O_3 (13-15 wt.%) can clearly establish their tholeiitic affinity. Clinopyroxene low Ti values (0.02 pfu.) for low Ca+Na (< 0.8 pfu) [Leterrier *et al.*, 1982], Mg enriched cores and Fe-rich rims, also establish that these clinopyroxene are tholeiitic (fig. 3). However, the relatively low whole rock MgO contents (< 7,5 wt.%) combined to the low Ni concentrations suggest that these magmas could have undergone fractionation dominated by olivine crystallisation.

The Nb/La vs. Ti/Y diagram shows that these Cuban dolerites are very similar in composition to the LTi Parana, Siberia, Deccan and Ethiopia flood basalts characterised by low TiO_2 (1.06 wt.% to 1.13 wt.% here) and P_2O_5 (0.08 wt.%) levels (fig.6) [Gibson *et al.,* 1995].

The multi-element concentrations of these dolerites are very similar to those in MORB (fig. 5) despite the low concentrations in Nb and Ta, typical of trapp formation [Thompson *et al.,* 1983], and bear a resemblance to trace-element diagrams of the Ferrar dolerites [Hergt *et al.*, 1989]. These differ from many other CFBs and display a marked negative Nb-Ta anomaly. This could reflect the existence of Nb-Ta bearing phases (magnetite) in the fractional crystallisation process or mark a form of crustal contamination, as suggested for other Mesozoic Gondwana CFB provinces [Peate *et al.,* 1996; Hansen *et al.*, 1999].

The ($^{208}Pb/^{204}Pb$)i and ($^{207}Pb/^{204}Pb$)i ratios of the dolerites sampled in the dyke cores suggest that the tholeiitic magma was contaminated by the upper continental crust. Differences in the chemistry from the core to the dyke-margins, marked by the high levels of Sr, Pb and Th and higher ($^{208}Pb/^{204}Pb$)i and ($^{207}Pb/^{204}Pb$)i ratios at the edge of a single dyke (fig. 8) suggest assimilation of the turbiditic sediments in contact with the dyke-margins. These sediments are derived from the erosion of the nearby North or South American continental plates and are known to have high Pb and Sr contents [Hauff *et al.*, 2000].

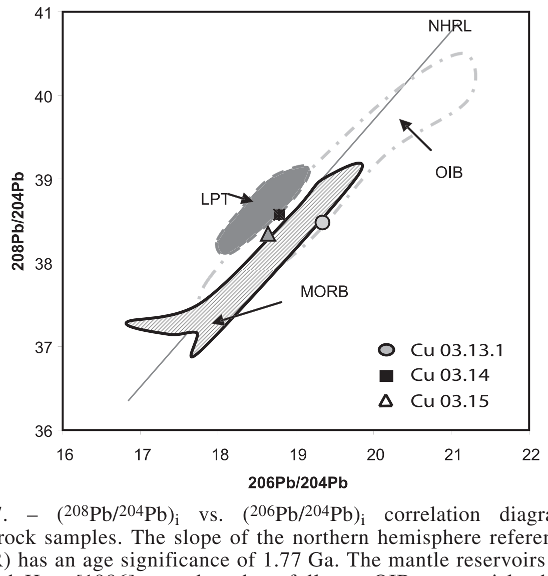

FIG. 7. – ($^{208}Pb/^{204}Pb$)$_i$ vs. ($^{206}Pb/^{204}Pb$)$_i$ correlation diagram for whole-rock samples. The slope of the northern hemisphere reference line (NHLR) has an age significance of 1.77 Ga. The mantle reservoirs of Zindler and Hart [1986] are plotted as follows: OIB: ocean island basalt; MORB: mid ocean ridge basalt; the LPT field (Low P_2O_5 and TiO_2) is from Hawkesworth *et al.* [1984].
FIG. 7. – *Diagramme* ($^{208}Pb/^{204}Pb$)$_i$ *vs.* ($^{206}Pb/^{204}Pb$)$_i$ *pour les échantillons Cu.03.13.1, Cu.03.14 et Cu.03.15. Les grands réservoirs magmatiques sont issus de Zindler et Hart [1986].* Le champ LPT (Low P_2O_5 *and* TiO_2) *a été défini par Hawkesworth* et al. *[1984].*

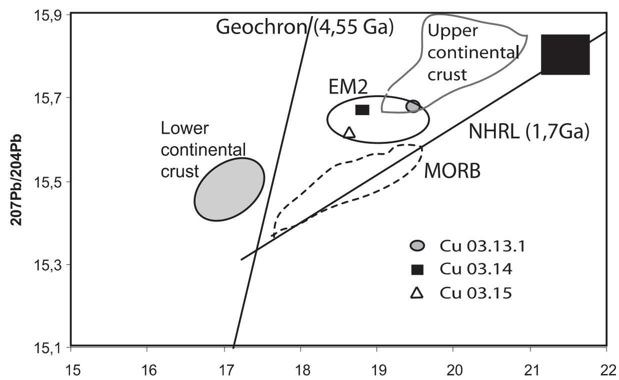

FIG. 8. – ($^{207}Pb/^{204}Pb$)i vs. ($^{206}Pb/^{204}Pb$)i correlation diagram for whole-rock samples. The mantle reservoirs of Zindler and Hart [1986] are plotted as follows: EM2: enriched mantle; HIMU: mantle with high U/Pb ratio.
FIG. 8. – *Diagramme* ($^{207}Pb/^{204}Pb$)$_i$ *vs.* ($^{206}Pb/^{204}Pb$)$_i$ *pour les échantillons Cu.03.13.1, Cu.03.14 et Cu.03.15. Les grands réservoirs magmatiques sont issus de Zindler et Hart [1986] : EM2 : enriched mantle; HIMU : manteau avec rapport U/Pb élevé.*

The high εNd values (+8.6 to +9.6) of the clinopyroxene separates and host rocks indicate that the dolerites derived from a depleted MORB-type mantle (DMM). Indeed, the εNd of the DMM at 150 Ma is +8.53 [($^{143}Nd/^{144}Nd$)I = 0,51288].

Continental flood basalts are related to mantle plumes, this can be seen by the similarities of HTi and OIB basalts [White and McKenzie, 1989; Pik *et al.*, 1998]. These authors suggest that LTi basalts originate from a HTi OIB-like source variably contaminated by the continental crust [Pik *et al.*, 1998]. The Ferrar magmatism [Hergt *et al.*, 1989; Peate *et al.*, 1996], and other magmatic events with similar geochemical characteristics such as basalt sequences in Antarctica and in Siberia [Storey and Alabaster, 1991; Lightfoot *et al.*, 1993], have been recognised as LTi basalt sequences. In these cases, the melt is much more depleted in incompatible elements than typical related OIB magmas [Anderson, 1994]. These Ferrar dolerites are interpreted as having been derived from mixing of a lithospheric mantle source and an asthenopheric component similar to E-MORB [Hergt *et al.*, 1989; Lightfoot *et al.*, 1993].

The MORB-like characteristics and the continental affinities of the three Cuban samples studied in this paper bear resemblance to the LTi continental flood basalts of Ferrar and to small volumetric basalt sequences of Antactica and Siberia [Hergt *et al.*, 1989; Lightfoot *et al.*, 1993; Storey and Alabaster, 1991].

These Cuban dolerites would owe their existence to the separation of the Yucatan block and South America linked to the opening of the Gulf of Mexico appreciatively 160 to 150 million years ago. This is correlated to the opening of the central Atlantic Ocean as suggested by previous authors [Kerr *et al.,* 1999; Duncan and Hargraves, 1984; Burke, 1988].

CONCLUSIONS

Mafic doleritic dykes intruding Jurassic turbidites of the El Sábalo formation belong to the Guaniguanico terrane, which represents a Jurassic-Cretaceous sequence of continental margin type. These Late Jurassic dolerites exhibit geochemical features of evolved tholeiitic melts, and more precisely of low TiO_2 and P_2O_5 (LTi) continental flood basalts similar to the dolerites of Ferrar. However, they differ from most continental flood basalt occurrences by LREE-depleted patterns similar to MORB, as well as by the small volume of erupted rocks. The dolerites and their clinopyroxenes, characterized by similar and high εNd values (+8.6 to +9.5) derived from mixing of a lithospheric mantle source and an asthenospheric component similar to E-MORB. The ($^{208}Pb/^{204}Pb$)i and ($^{207}Pb/^{204}Pb$)i ratios of the dolerites sampled in the dyke cores suggest that the tholeiitic magma has been contaminated by the upper continental crust whereas the high levels in Sr, Pb and Th and higher ($^{208}Pb/^{204}Pb$)i and ($^{207}Pb/^{204}Pb$)i ratios of the chilled margin of a single dyke suggest assimilation of the host Jurassic sediments. These 165-150 Ma doleritic dykes were emplaced during the separation of the Yucatan block from South America and could reflect the opening of the Gulf of Mexico.

Acknowledgements. – This study was initiated by our late colleague and co-author Henriette Lapierre, a passionate geologist; she was a friend to all of us. We are indebted to our Cuban co-author for her field assistance, for permitting us to collect samples and granting us permission to remove them from her country. We thank R. Maury and S. Guillot for their valuable help to improve the manuscript.

References

ANDERSON D.L. (1994). – Komatiites and picrites: evidence that plume source is depleted. – *Earth Planet. Sci. Lett.,* **128,** 303-311.

BARRAT J.A, KELLER F. & AMOSSE J. (1996). – Determination of the rare earth elements in sixteen reference samples by ICP-MS after Tm addition and ion exchange separation. – *Geostand. Newslett.*, **20**, 133-139.

BLEIN O., GUILLOT S., LAPIERRE H., MERCIER DE LEPINAY B., LARDEAUX J.-M., MILLAN TRUJILLO G., CAMPOS M. & GARCIA A. (2003). – Geochemistry of the Mabujina complex, Central Cuba: implications on the Cuban Cretaceous arc rocks. – *J. Geol.*, **111**, 89-101.

BURKE K. (1988). – Tectonic evolution of the Caribbean. – *Ann. Rev. Earth Planet. Sci. Lett.*, **16**, 201-230.

COTTEN J., LE DEZ A., BAU M., CAROFF M., MAURY R.C., DULSKI P., FOURCADE S., BOHN M. & BROUSSE R. (1995). – Origin of an anomalous rare-earth element and yttrium enrichments in sub aerially exposed basalts: evidence from French Polynesia. – *Chem. Geol.,* **119**, 115-138.

DUNCAN R.A. & HARGRAVES R. B. (1984). – Plate tectonic evolution of the Caribbean region in the mantle reference frame. *In*: BONINI W.E., HARGRAVES R.B. & SHAGAM R., Eds, The Caribbean-South American plate boundary and regional tectonics. – *Mem. Geol. Soc. Amer.*, vol. **162**, 81-93.

GIBSON S.A., THOMPSON R.N., DICKIN A.P. & LEONARDOS O.H. (1995). – High-Ti and low-Ti potassic magmas: key to understanding plume-lithosphere interactions and continental flood basalt genesis. – *Earth Planet. Sci. Lett.,* **136**, 149-165.

HANSEN H. & NIELSEN T.F.D. (1999). – Crustal contamination in Palaeogene East Greenland flood basalts: plumbing system evolution during continental rifting. – *Chem. Geol.*, **157**, 89-118.

HAUFF F., HOERNLE G., TILTION G., GRAHAM W. & KERR A.C. (2000). – Large volume recycling of oceanic lithosphere over short time scales: geological constraints from the Caribbean large igneous Province. – *Earth Planet. Sci. Lett*., **174**, 247-263.

HAWKESWORTH C.J., MARSH J.S., DUNCAN A.R., ERLANK A.J. & NORRY M.J. (1984). – The role of continental lithosphere in the generation of the Karoo volcanic rocks: evidence from combined Nd and Sr isotope studies. – *Spec. Publ. Geol. Soc. S. Africa*, **13**, 341-354.

HERGT J.M., CHAPPELL B.W., MCCULLOGH M.T., MCDOUGALL T. & CHIVAS A.R. (1989). – Geochemical and isotopic constaints on the origin of the Jurassic dolerites of Tasmania. – *J. Petrol*., **30**, 841-883.

HOFMANN A.W (1988). – Chemical differentiation of the Earth: the relationship between mantle, continental crust, and oceanic crust. – *Earth Planet. Sci. Lett.,* **90**, 297-314.

ITURRALDE-VINENT M.A. (1994). – Cuban geology: a new plate tectonics synthesis. – *J. Petro. Geol.,* **17**, 39-70.

ITURRALDE-VINENT M.A. (1996a). – Introduction to Cuban geology and geophysics. *In*: M.A. ITURRALDE-VINENT, Ed., Cuban ophiolites and volcanic arcs. – *Miami, Fla, Int. Geol Correlation Program,* **364**, 179-211.

ITURRALDE-VINENT M.A. (1996b). – El arco de islas volcanicas del Cretacico. Introduction to Cuban geology and geophysics. *In*: M.A. ITURRALDE-VINENT, Ed., Cuban ophiolites and volcanic arcs. – *Miami, Fla, Int. Geol Correlation Program*

ITURRALDE-VINENT M.A. (1998). – Introducción a la geología de Cuba. *In*: G. FURRAZOLA BERMÚDEZ and K. NÚNEZ CAMBRA, Eds, Estudios sobre geologia de Cuba, La Habana. – Centro Nacional de Informacion Geologica, 35-68.

KERR A.C., TARNEY J., MARRINER G.F., NIVIA A., KLAYER G.T. & SAUNDERS A.D. (1996). – The geochemistry and tectonic setting of Late Cretaceous Caribbean and Colombian volcanism. – *J. South Am. Earth Sci*., **9**, 111-120.

KERR A.C., TARNEY J., MARRINER G.F., NIVIA A. & SAUNDERS A.D. (1997). – The Caribbean-Colombian igneous Province: the internal anatomy of an oceanic plateau. – *Geophys. Monogr.*, **100**, 123-144.

KERR A.C., ITURRALDE-VINENT M.A., SAUNDERS A.D., BABBS T.L. & TARNEY J. (1999). – A new plate tectonics model of the Caribbean: implications from a geochemical reconnaissance of Cuban Mesozoic volcanic rocks. – *Geol. Soc. Amer. Bull.,* **111**, 11, 1581-1599.

LAPIERRE H., DUPUIS V., MERCIER DE LEPINAY B., TARDY M., RUIZ J., MAURY R.C., HERNANDEZ J. & LOUBET M. (1997). – Is the Lower Duarte Igneous Complex (Hispaniola) a remnant of the Caribbean plume-generated oceanic plateau? – *J. Geol*., **105**, 111-120.

LAPIERRE H., BOSCH D., DUPUIS V., POLVE M., MAURY R.C., MAURY R.C., HERNANDEZ J., MONIE P., YEGUICHEYAN D., TARDY M., MERCIER DE LEPINAY B., MAMBERTI M., DESMET A., KELLER F. & SENEBIER F. (2000). – Multiple plume events in the genesis of the peri-Caribbean Cretaceous oceanic plateau province. – *J. Geol. Res.,* **105**, 8403-8421.

LE MAITRE R.W., BATEMAN P., DUDEK A., KELLER J., LAMEYRE LE BAS M. J., SABINE P.A., SCHMIDT R., SORENSEN H., STRECKEISEN A., WOOLLEY A.R. & ZANETTIN B. (1989). – A classification of igneous rocks and glossary terms. – Blackwell. Oxford.

LETERRIER J., MAURY R.C., THONON P., GIRARD D. & MARCHAL M. (1982). – Clinopyroxene composition as a method of identification of the magmatic affinities of paleo-volcanic series. – *Earth Planet. Sci. Lett.,* **59**, 139-154.

LIGHTFOOT P.C., HAWKESWORTH C.J., HERGT G.M., NALDRETT A.J., GORBACHEV N.S., FEDORENKO V.A. & DOHERTY W. (1993). – Remobilisation of the continental lithosphere by a mantle plume: major-, trace-element, and Sr-, Nd- and Pb- isotope evidence from picritic and tholeiitic lavas of Noril'sk District, Siberian Trap, Russia. – *Contrib. Min. Pet*., **114**, 171-188.

MARESCH W., STOCKHERT B., BAUMANN A., BRIX S., THOMSON C., KAISER C., KLUGE R. & KRUCKHANS-LUEDER G. (2000). – Crustal history and plate tectonic development in the southern Caribbean. – *Zeitschrift für Angewandte Geologie*, SH1.

MCCULLOCH M.T. & WASSERBURG T.H. (1978). – Sm-Nd and Rb-Sr chronology of continental crust formation. – *Sciences*, **200**, (4345), 2003-2011.

MESCHEDE M. & FRISCH W. (1998). – A plate-tectonic model for the Mesozoic and early Cenozoic history of the Caribbean plate. – *Tectonophysics,* **296**, 269-291.

MESCHEDE M. & FRISCH W. (2002). – The evolution of the Caribbean plate and its relation global plate motion vectors: Geometric constraints for an inter-American origin. *In*: T.A. JACKSON Ed., Caribbean geology into the Third Millennium: *Transactions of the Fifteenth Caribbean Geological Conference*. – University of the West Indies press, –14.

MIDDLEMOST E.A.K. (1975). – The basalt clan. – *Earth Sci. Rev*., **11**, 337-364.

MORIMOTO N., FABRIES J., FERGUSON A., GINZBURG I., ROSS M., SEIFERT F. & ZUSSMAN J. (1988). – Nomenclature of pyroxenes. – *Bull. Mineral.,* **111**, 535-550.

MULLER R.D., ROYER J-Y. CANDE S.C., ROEST W.R. & MASCHENKOV S. (1999). – New constraints on the Late Cretaceous/Tertiary plate tectonic evolution of the Caribbean. *In*: P. MANN Ed., Caribbean basins, sedimentary basins of the World. – Elsevier Science, B.V., Amsterdam, the Netherlands, 33-59.

PEATE D.W. & HAWKESWORTH C.J. (1996). – Lithospheric to asthenospheric transition in low-Ti flood basalts from southern Parana, Brazil. – *Chem. Geol*., **127**, 1-24.

PIK R., DENIEL C., COULON C., GEZAHEGN Y., HOFMAN C., AYALEW D. & ROLLINSON H. (1998). – The northwestern Ethiopian plateau flood basalts: Classification and spatial distribution of magma types. – *J. Volcanol. Geotherm. Res*., **81**, 91-111.

PSZCZOLKOWSKI A. (1978). – Geosynclinal sequences of the Cordillera de Guaniguanico in western Cuba: their lithostratigraphy, facies development and paleogeography. – *Acta Geol. Polonica,* **28**, 1-96.

REGUERA COBIELLA J.L. & CRUZ GAMEZ E.M. (1999). – Geocuba, espacios naturales y geología Cubana. – Monografías de Enseñanza de las Ciencias de la Tierra, Asociacíon Española para la Enseñanza de las Ciencias de la Tierra, Universidad de Pinar del Rio Cuba, 79 pp.

RODRÍGUEZ ARCIA M., RODRÍGUEZ BARRANCO G., ALVAREZ DEL BUSTO R., PEREZ CANETE C.C., RODRÍGUEZ COTILLA M.O., GONZALEZ CLEMENTE E.C., GUTIEREZ DOMECH R., HERNANDEZ SANTANA J.R., PEREZ INTERIAN S., MARQUES TABLON M.E., RODRIGUEZ MATEO J., GUTIEREZ MUNIZ O., RABASA PALET M., FRAGEMIL PROPIN E. & VALDES C. (1997). – Generalidades de la geología de Cuba. *In*: G.F. BERMÚDEZ FURRAZOLA and K.E. CAMBRA NÚNEZ Eds, Estudios sobre geología de Cuba. – Instituto de Geología y Paleontología, Ciudad de la Habana, Cuba, 13-68.

SCHNEIDER J., BOSCH D., MONIE P, GUILLOT S., GARCIA-CASCO A.G., LARDEAUX J.M., TORRES-ROLDAN R.L. & MILLAN T. (2004). – Origin and evolution of the Escambray massif (central Cuba): an example of HP/LT rocks exhumed during intraoceanic subduction. – *J. Metam. Geol.,* **22**, 227-247.

SINTON C.W., DUNCAN R.A., STOREY M., LEWIS J. & ESTRADA J.J. (1998). – An oceanic flood province within the Caribbean plate. – *Earth Planet. Sci. Lett*., **155**, 221-235.

STANEK K.P., COBIELLA-REGUERA J.L., MARESCH W.V., MILLAN TRUJILLO G.M., GRAFE F. & GREVEL C. (2000). – Geological development of Cuba. – *Zeitschrift für Angewandte Geologie,* **SH1**, 259-265.

STOREY B.C. & ALABASTER T. (1991). – Tectonomagmatic controls on Gondwana break-up models: evidence from proto-pacific margin of Antarctica. – *Tectonics*, **10**, 1274-1288.

SUN S.S. & MCDONOUGH W.F. (1989) – Chemical and isotopic systematics of ocean basalts: implications for the mantle compositions and processes. *In*: A.D. SAUNDERS and M.G. NORRY, Eds, Magmatism in ocean basins. – *Geol. Soc. London Sp. Publ.,* **42**, 313-345.

THOMPSON R.N., MORRISSON M.A., DICKIN A.P. & HENDRY G.L. (1983). – Continental flood basalts… Arachnids rule OK? *In*: C.J. HAWKESWORTH & M.J. NORRY, Eds., Continental basalts and mantle xenoliths. – Shiva, Nantwich, UK, 158-185.

TODT W., CLIFF R.A., HANSER A. & HOFMANN A.W. (1996). – Evaluation of a ^{202}Pb-^{205}Pb double spike for high precision lead isotope analysis. *In*: A. BASU and S. HART Eds, Earth processes: reading the isotopic code. – AGU, Washington, D.C., 429-437.

WHITE M.W., ALBAREDE F. & TELOUK F. (2000). – High-precision analysis of Pb isotopic ratios by multi-collector ICP-MS. – *Chem. Geol.,* **167**, 257-270.

WHITE R.S. & MCKENZIE D.P. (1989). – Magmatism at rift zones: the generation of volcanic continental margins and flood basalts. – *J. Geophys. Res*., **94**, 7685-7730.

ZINDLER A. & HART S.R. (1986). – Chemical geodynamics. – *Ann. Rev. Earth Planet. Sci. Lett*., **14**, 493-571.